

## Original Article

# RUNX3 derived hsa\_circ\_0005752 accelerates the osteogenic differentiation of adipose-derived stem cells via the miR-496/MDM2-p53 pathway

Ming Wang<sup>a, b</sup>, Yifan Huan<sup>c</sup>, Xiyang Li<sup>c</sup>, Jing Li<sup>a</sup>, Guohua Lv<sup>a, \*</sup><sup>a</sup> Department of Spine Surgery, The Second Xiangya Hospital of Central South University, Changsha 410011, Hunan Province, PR China<sup>b</sup> Department of Spine Surgery, The First Affiliated Hospital of University of South China, Hengyang 421001, Hunan Province, PR China<sup>c</sup> Department of Orthopedics, Financial and Trade Hospital of Hunan Province, Changsha 410001, Hunan Province, PR China

## ARTICLE INFO

## Article history:

Received 20 August 2021

Received in revised form

17 September 2021

Accepted 21 September 2021

## Keywords:

RUNX3

Adipose-derived stem cells

Osteogenic differentiation

Circular RNAs

microRNA

MDM2

## ABSTRACT

**Background:** Circular RNAs (circRNAs) are non-coding RNAs that play a pivotal role in bone diseases. RUNX3 was an essential transcriptional regulator during osteogenesis. However, it is unknown whether RUNX3 regulates hsa\_circ\_0005752 during osteogenic differentiation.

**Methods:** The levels of hsa\_circ\_0005752 and RUNX3 were measured by qRT-PCR after osteogenic differentiation of ADSCs. The osteogenic differentiation was analyzed by Alkaline phosphatase (ALP) staining and Alizarin red staining (ARS). qRT-PCR and western blot were used to assess the expressions of osteogenic differentiation-related molecules. RNA pull-down, RIP, and luciferase reporter assays determine the interactions between miR-496 and hsa\_circ\_0005752 or MDM2 mRNA. CHIP-PCR analyzed the interaction between RUNX3 and LPAR1. Finally, the potential roles of RUNX3 were investigated during osteogenic differentiation with or without hsa\_circ\_0005752 knockdown.

**Results:** Hsa\_circ\_0005752 and RUNX3 were significantly increased, and miR-496 was remarkably decreased in ADSCs after osteogenic differentiation. Hsa\_circ\_0005752 could promote osteogenic differentiation, as shown by enhancing ALP and ARS staining intensity. Hsa\_circ\_0005752 enhanced the expressions of Runx2, ALP, Osx, and OCN. Furthermore, hsa\_circ\_0005752 directly targeted miR-496, which can directly bind to MDM2. RUNX3 bound to the LPAR1 promoter and enhanced hsa\_circ\_0005752 expressions. Moreover, the enhanced expression of hsa\_circ\_0005752 by RUNX3 could promote osteogenic differentiation, whereas knockdown of hsa\_circ\_0005752 partially antagonized the effects of RUNX3.

**Conclusion:** Our study demonstrated that RUNX3 promoted osteogenic differentiation via regulating the hsa\_circ\_0005752/miR-496/MDM2 axis and thus provided a new therapeutic strategy for osteoporosis. © 2021, The Japanese Society for Regenerative Medicine. Production and hosting by Elsevier B.V. This is an open access article under the CC BY-NC-ND license (<http://creativecommons.org/licenses/by-nc-nd/4.0/>).

**Abbreviations:** Runx3, RUNX Family Transcription Factor 3; LPAR1, lysophosphatidic acid receptor 1; circRNAs, Circular RNAs; miRNAs, microRNA; ADSCs, adipose-derived stem cells; OM, osteogenic (differentiation) medium; MDM2, murine double minute 2; Runx2, Runt-related transcription factor 2; ALP, alkaline phosphatase; ARS, Alizarin Red Staining; OCN, osteocalcin; Osx, osterix; BM-MSCs, Bone Marrow-Mesenchymal Stem Cells; UC-MSCs, Umbilical Cord-Mesenchymal Stem Cells; BMP2, Bone morphogenetic protein 2; 3' UTR, 3' untranslated region; qRT-PCR, quantitative real-time polymerase chain reaction; ChIP, chromatin immunoprecipitation; PMSF, phenylmethylsulfonyl fluoride; BCA, bicinchoninic acid; SDS-PAGE, polyacrylamide gel electrophoresis; ECL, enhanced chemiluminescence; RIP, RNA immunoprecipitation; H&E staining, Hematoxylin and Eosin staining.

\* Corresponding author. Department of Spine Surgery, The Second Xiangya Hospital of Central South University, NO. 139, Renmin Middle Road, Changsha 410001, Hunan Province, PR China.

E-mail address: [wmspine@163.com](mailto:wmspine@163.com) (G. Lv).

Peer review under responsibility of the Japanese Society for Regenerative Medicine.

<https://doi.org/10.1016/j.reth.2021.09.006>

2352-3204/© 2021, The Japanese Society for Regenerative Medicine. Production and hosting by Elsevier B.V. This is an open access article under the CC BY-NC-ND license (<http://creativecommons.org/licenses/by-nc-nd/4.0/>).

## 1. Introduction

Osteoporosis contributes a lot to bone fractures and bone-related morbidities and mortalities in women and men [1]. The features of osteoporosis were the decreased bone mass and bone mineral density, further decreasing bone strength and increased bone fragility. The causes for osteoporosis are multifactorial, but the primary etiology is abnormal bone resorption and formation [2]. Hence, the molecular mechanisms underlying bone remodeling by promoting osteogenic differentiation will bring out a new light on the therapeutics of osteoporosis. Currently, there are several types of adult stem cells, including Bone Marrow-Mesenchymal Stem Cells (BM-MSCs), which were the cell source for stem cell-based therapies [3]. Considering the painful harvesting process and limited source, we found ADSCs own the most abundant source for transplantation compared with the other two cell types [3,4]. Also, adipose-derived stem cells (ADSCs) own self-renewal and differentiation abilities into many cells, including osteoblasts [4,5]. These advantages enable ADSCs to be attractive cells for clinical bone regeneration and repair. Nevertheless, the mechanisms of osteogenic differentiation of ADSCs are limited.

Runt-related transcription factor 3 (RUNX3) was involved in many diseases, such as cancers [6], inflammation [7], and neuropathy [8]. The previous report pointed out that RUNX3 was a DNA-binding transcription factor, which participates in cell proliferation, differentiation, and cell lineage specification [9]. Recently, experiments validated that RUNX3 modulates the chondrocyte proliferation and differentiation through downregulating SOX9 expression [10], and endothelial progenitor cell differentiation [11], indicating that RUNX3 was a vital regulator for lineage differentiation. However, until now, the role of RUNX3 in osteogenic differentiation remains elusive.

Circular RNAs (circRNAs) are mainly produced by back-splicing events [12], which play an essential regulatory role during the normal development of tissues or organs and the pathophysiological process of diseases [12,13]. As a miRNA sponge, circRNAs influence the binding of miRNAs to mRNAs directly and further influence the target gene expression [14,15]. Recently, several reports showed circRNAs were involved in the osteoporotic developmental process by influencing osteogenic differentiation. For example, circRNA\_0016624 could bind to miR-98 and promote osteogenic differentiation by upregulating BMP2 [16]. In addition, CircRNA\_33287 promoted osteogenic differentiation through the miR-214-3p/Runx3 pathway [17]. A recent study using circRNA microarray showed that hsa\_circ\_0005752 was significantly upregulated during human ADSC (hADSC) osteogenic differentiation, which meant hsa\_circ\_0005752 might be a crucial regulator in the osteogenic differentiation of ADSCs [18]. However, it is still primarily unknown about the functional roles and definite mechanisms of hsa\_circ\_0005752 during osteogenic differentiation of ADSCs.

Previous studies pointed out circRNAs regulated gene expression by modulating the alternative splicing of the target gene or as a miRNA sponge to influence the expression of downstream mRNA or acting on RNA binding protein to regulate the parental transcription gene [13,15]. Using the bioinformatics method by circular RNA Interactome (<https://circinteractome.nia.nih.gov/index.html>), we found hsa\_circ\_0005752 had a potential binding site for miR-496. However, whether hsa\_circ\_0005752 plays a role in osteogenic differentiation through miR-496 is needed to be validated.

Murine double minute 2 (Mdm2) is the principal protein for the specific degradation of the p53 protein [19,20]. Previous studies indicated that Mdm2 regulated cellular differentiation,

such as osteoblast [21,22], myoblasts [23,24], and odontoblasts [20]. Additionally, it was confirmed that MDM2 regulated stem cell differentiation by regulating the ubiquitination and subsequent degradation of p53, thus influencing p53-dependent transcriptional activities [19]. Recent studies showed that MDM2-p53 signaling was a critical pathway to controlling and maintaining osteoblast differentiation and skeletal development. Knockdown of MDM2 in osteoblast progenitor cells increased p53 activities and decreased the osteogenic differentiation and the levels of osteoblast transcriptional regulator Runx2. In contrast, p53 mutant osteoblast progenitor cells exhibited increased cell proliferation and the expression of Runx2 and promoted osteoblast maturation [21]. Using starBase (<http://starbase.sysu.edu.cn/>), we found that MDM2 is potentially bound to miR-496. Hence, we proposed that miR-496 modulates ADSCs osteogenic differentiation, possibly by regulating the MDM2-p53 axis. Here, we investigated the role and the possible mechanisms by which circRNA hsa\_circ\_0005752 regulated the ADSC osteogenic process, which holds great promise of a new therapeutic strategy for osteoporosis.

## 2. Materials and methods

### 2.1. Cell culture and osteogenic differentiation

The ADSCs were purchased from Procell (CP-H202) and maintained in the ADSCs growth medium (Cat # MD-0003) at 37 °C with 5% CO<sub>2</sub>/95% O<sub>2</sub>. Cells at 3–5 passages were used for all the experiments. After cells reached about 80% confluence, the growth medium was aspirated, and cells were washed with PBS. Then, the ADSCs were cultured in an osteogenic differentiation medium (OM) (Cyagen Biosciences, HUXMD-90021) for inducing osteogenic differentiation.

### 2.2. Lentivirus infection and cell transfection

Lentivector-mediated short-hairpin hsa\_circ\_0005752 (sh-hsa\_circ\_0005752), short-hairpin MDM2 (sh-MDM2), short-hairpin RUNX3, and the corresponding scrambled control (sh-NC), pcDNA3.1-RUNX3, and its empty vector pcDNA3.1 were provided by GenePharma Company (Shanghai, China). We purchased recombinant lentiviruses containing full-length hsa\_circ\_0005752 and the corresponding scrambled control (vector) from GenePharma Company. OptiMEM (Invitrogen Carlsbad, CA, USA) and 5 mg/mL polybrene were used for the lentivirus transfection with an optimized volume of virus supernatant.

We purchased miR-496 mimics and inhibitors and their corresponding negative controls (mimic/inhibitor NC) from GenePharma (Shanghai, China). For transfection, plasmids were transfected into ADSCs using Lipofectamine 3000 (Invitrogen; Carlsbad, CA, USA). Forty-eight hours after transfection, we harvested the cells for subsequent experiments. The individual experiment was performed at least three times.

### 2.3. ALP staining

We purchased the commercial BCIP/NBT staining kit from Biotechnology Co., Ltd. (Shanghai, China). ALP staining was performed according to the protocol. Briefly, ADSCs were cultured in an osteoblastic induction medium for seven days. Then the medium was gently discarded, and cells were washed with 1 × PBST once. The cells were fixed with 4% paraformaldehyde at room temperature for 30min.

#### 2.4. Alizarin Red Staining (ARS)

After 14-day osteogenic induction of ADSCs, the cells were fixed by 95% ethanol and stained with 0.1% ARS (pH 4.2; Sigma-Aldrich, MO, USA) for 20 min. Then, cells were washed with distilled water. To exhibit the mineralized nodules, we used 10% cetylpyridinium chloride (Sigma-Aldrich, MO, USA) to dissolve the stain for 1 h. The absorbance was detected by spectrophotometry. Protein concentrations normalized the ARS intensity.

#### 2.5. Quantitative real-time polymerase chain reaction (qRT-PCR)

After osteogenic differentiation of ADSCs, total RNA was extracted using the Qiagen RNeasy Mini Kit (Qiagen). After determination of the quality and concentration by a NanoDrop 2000 Spectrophotometer (Thermo Fisher Scientific), 1 µg of total RNA was used to synthesize cDNA using a PrimeScript RT Reagent Kit (TaKaRa, Dalian, China). The expressions of circRNA hsa\_circ\_0005752, MDM2, or miR-496 were detected by the SYBR Premix Ex Taq kit (Takara) or TaqMan™ MicroRNA Assay (Thermo Fisher Scientific). β-actin or U6 was used as an internal control. PCR procedure was performed on the Rotor-Gene Q (Qiagen). We used the  $2^{-\Delta\Delta Ct}$  method to calculate the relative expression. Primer sequences were listed below: hsa\_circ\_0005752 primers, F 5'-CTCTTCAGTTGCACTTAATCAGC-3', R 5'-ACCTGGCCGATGAAGATAGAG-3'. MDM2 primer, F: 5'-GGCAGGGGAGAGTGATACAGA-3', R 5'-GAAGCCAATTCTCACGAAGGG-3'. RUNX3 primer, F: 5'-AGGCAATGACGAGAACTACTCC-3', R 5'-CGAAGTTCGTTGAACCTGG-3'. β-actin primer, F: 5'-CCCTGGAGAAGAGCTACGAG-3', R 5'-CGTACAGGCTTTGCGGATG-3'. miRNA-496 primer, F: 5'-GCCGTGAGTATTACATGGCC-3', R: 5'-CTCAACTGGTGTCTGGAGTC-3'. U6 primer: F: 5'-GAGACGGGAACGACAAACCT-3', R: 5'-TGGACGAA-GAGGATTCGCTG-3'.

#### 2.6. Western blot analysis

ADSCs were lysed by RIPA buffer containing 1 mM Phenylmethylsulfonyl fluoride (PMSF, Sigma-Aldrich). After clearance at 12,000 g for 15 min, the supernatant was collected. Protein concentration was measured using a Pierce™ BCA Protein Assay Kit (Thermo Fisher Scientific). 20 µg of total protein was separated by 10% SDS-PAGE (sodium dodecyl sulfate-polyacrylamide gel electrophoresis) and transferred to nitrocellulose membranes. After three washes by 1 × TBST (Tris-buffered saline with 0.1% Tween® 20), the membrane was blocked for 2 h by 5% non-fat milk in 1 × TBST. The individual primary antibodies were applied to the membrane at 4 °C overnight. The primary antibodies were mouse anti-MDM2 (ab16895, Abcam), rabbit anti-p53 (ab227655, Abcam), mouse anti-Runx2 (ab76956, Abcam), rabbit anti-Osx (ab227820, Abcam), rabbit anti-RUNX3 (ab224641, Abcam), rabbit anti-LPAR1 (BS-2880R, Thermo Fisher Scientific), rabbit anti-β-actin (ab8227, Abcam). After three washes by 1 × TBST, the individual horseradish peroxidase (HRP)-labeled secondary antibody was added according to the corresponding primary antibody. The secondary antibodies used were donkey anti-rabbit IgG H&L (ab207999, Abcam) and donkey anti-mouse IgG H&L (ab208001, Abcam). Following three washes with 1 × TBST, the membranes were developed by Super-Signal™ & Pierce™ ECL (Thermo Fisher Scientific, Illinois, USA) and imaged by Image Lab™ 4.1 (Bio-Rad).

#### 2.7. RNA pull-down

The pull-down assay of hsa\_circ\_0005752 was performed by biotin-coupled miR-496. Briefly, 20 nM of 3'-biotinylated- miR-

496 (miR-496 mimic), 3'-biotinylated-MUT miR-496 (MUT-miR-496 mimic), and bio-miR- scramble mimics (mimic NC) were transfected into ADSCs using Lipofectamine 3000. At 48 h after transfection, the cells were lysed for subsequent pull-down assay through incubating the cell lysate with 20 µL Dynabeads M-280 Streptavidin beads (Life Technologies, 11206D). The bound RNA was extracted using an RNeasy Mini Kit (QIAGEN) and dissolved in 25 µL of nuclease-free water. Nanodrop determined RNA concentration. 50 ng of total RNA was used to synthesize the cDNA. The qRT-PCR detected the abundance of hsa\_circ\_0005752 in the RNA complex.

#### 2.8. RNA immunoprecipitation (RIP)

Forty-eight hours after transfection of miR-496 mimics or mimic NC, the cells were harvested, and RIP was performed according to the EZ-Magna RIP kit (Millipore) by the detailed protocol using anti-argonaute 2 (AGO2) or control anti-IgG antibody. The purified RNA was extracted from the RNA-protein complex using an RNeasy Mini Kit (Qiagen). 50 ng of total RNA was reversely transcribed into cDNA, and an SYBR Green PCR kit (Takara) analyzed the level of hsa\_circ\_0005752 or MDM2 mRNA using a Rotor-Gene Q (Qiagen).

#### 2.9. Dual-luciferase reporting assay

Hsa\_circ\_0005752 were detected and identified using circBase (<http://www.circbase.org/>). The potential miR-496 binding sites for hsa\_circ\_0005752 or target genes were predicted using Circular RNA Interactome (<https://circinteractome.nia.nih.gov/index.html>) and starBase (<http://starbase.sysu.edu.cn/>). hTFtarget (<http://bioinfo.life.hust.edu.cn/hTFtarget>) found RUNX3 was a potential upper transcription factor for LPAR1. To determine the interaction between miR-496 and hsa\_circ\_0005752 or MDM2, between RUNX3 and LPAR1, the putative target sequences of miR-496 in hsa\_circ\_0005752, MDM2 and the corresponding mutation, and the potential binding sequence of RUNX3 in LPAR1 promoter region were cloned into luciferase vector pGL4.32 (Promega, WI, USA). The constructs are WT- hsa\_circ\_0005752, MUT-hsa\_circ\_0005752, WT-MDM2, MUT-MDM2, and pGL4.32-LPAR1. For the luciferase assay, ADSCs were co-transfected with (1) WT- hsa\_circ\_0005752 or MUT-hsa\_circ\_0005752 together with the miR-496 mimics or mimic NC; (2) WT-MDM2 or MUT-MDM2 together with the miR-496 mimics or mimic NC; (3) pcDNA3.1 empty vector, pcDNA3.1-RUNX3, sh-NC or sh-RUNX3 together with the pGL4.32-LPAR1. Lipofectamine 3000 (Invitrogen) was used to perform the transfection according to the manufacture's protocol. Forty-eight hours after transfection, the luciferase activity was detected using the dual-luciferase reporter assay system (Promega, WI, United States).

#### 2.10. Chromatin immunoprecipitation (ChIP)

ChIP assay was performed using a commercial kit 17-10086, EMD Millipore, GER). 1 × 10<sup>7</sup> ADSCs were cross-linked in 1% formaldehyde (Sigma, Catalog # 252549) and treated with 125 mM glycine. After washing by cold PBS, the cells were subjected to the lysis buffer containing protease inhibitors on ice for 10 min. After sonication and centrifugation, the pellet was re-dissolved in 1 mL of nuclear lysis buffer. The lysates were incubated with an anti-RUNX3 antibody (ab224642, Abcam) or Normal IgG (ab172730, Abcam). Then, the immunoprecipitated DNA was extracted from the DNA-protein complex, the enrichment of the LPAR1 promoter was analyzed by qPCR.

2.11. Statistical analysis

Results were shown as means ± standard deviations (SDs). The statistical analyses were performed using GraphPad Prism 6.0. One-way ANOVA was used to analyze the difference among the multiple groups. The student's *t*-test was used to evaluate the difference between two groups among multiple groups. *P* < 0.05 was regarded as statistical significance.

3. Results

3.1. Hsa\_circ\_0005752 promoted osteogenic differentiation of ADSCs

We firstly evaluated hsa\_circ\_0005752 levels during the process of osteogenic differentiation. Our qRT-PCR results showed that compared with day 0, the expression of hsa\_circ\_0005752 was

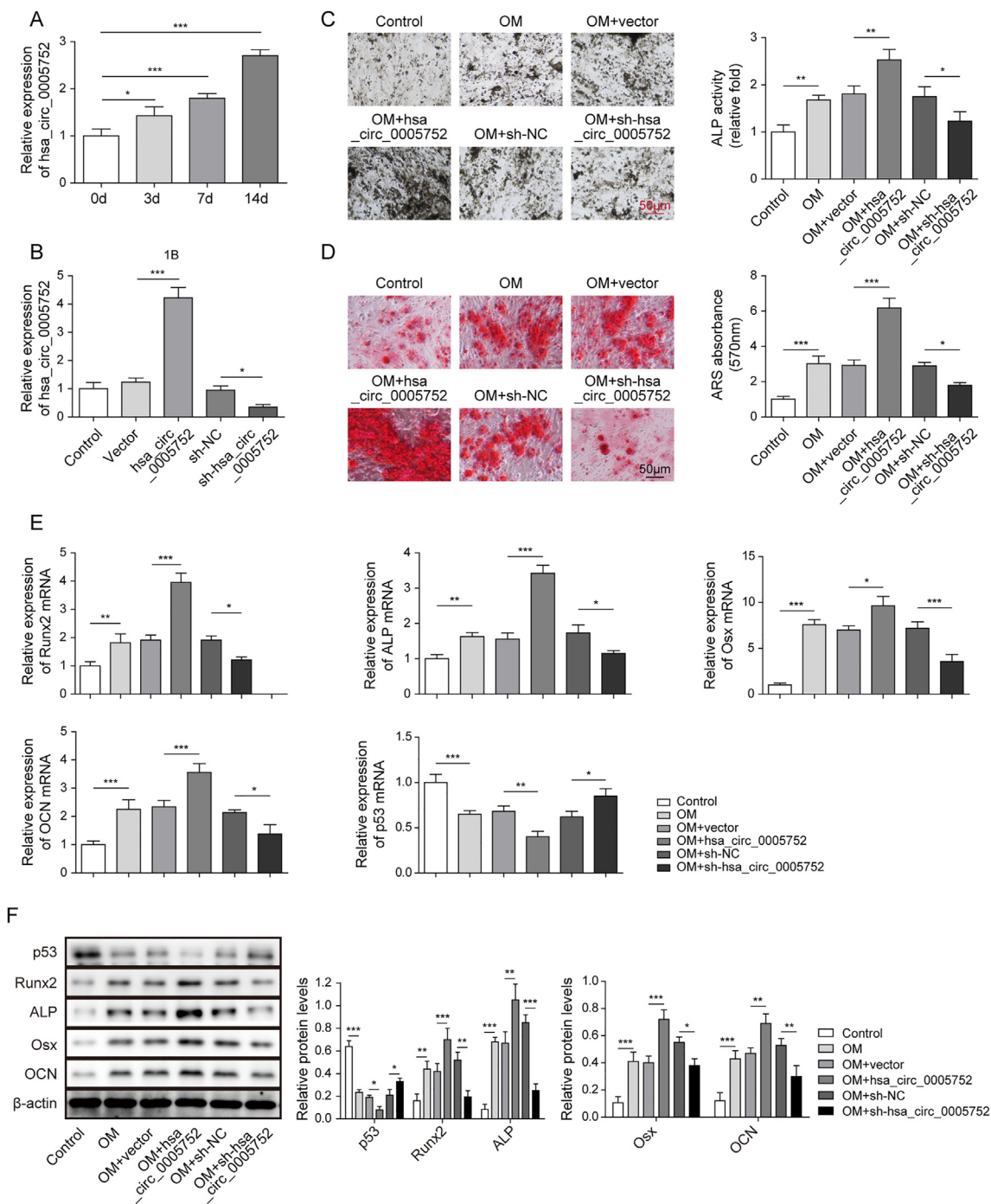


**Fig. 1. Hsa\_circ\_0005752 promoted osteogenic differentiation of ADSCs.** A: Hsa\_circ\_0005752 levels were determined by qRT-PCR in ADSCs during osteogenic differentiation at 0, 3, 7, and 14 days. B: Hsa\_circ\_0005752 was measured by qRT-PCR after transfections of hsa\_circ\_0005752, sh-hsa\_circ\_0005752, or their corresponding control. C–D: Alkaline phosphatase (ALP) or the mineralization was determined by the ALP staining (C) or Alizarin Red S (ARS) staining (D). Scale bar = 50 μm. E–F: Runx2, ALP, Osx, OCN, and p53 mRNA levels were determined by qRT-PCR (E) or Western blot (F) in OM-treated ADSCs after hsa\_circ\_0005752 overexpression or knockdown. Data indicated the mean ± SD, n = 3. \**P* < 0.05, \*\**P* < 0.01, \*\*\**P* < 0.001.

markedly increased after OM induction in a time-dependent manner (Fig. 1A). Next, we transfected pcDNA3.1-hsa\_circ\_0005752 and sh-hsa\_circ\_0005752 vector into ADSCs to achieve hsa\_circ\_0005752 overexpression or knockdown cells. The result revealed that the transfection of pcDNA3.1-hsa\_circ\_0005752 upregulated hsa\_circ\_0005752, and the transfection of sh-hsa\_circ\_0005752 induced the downregulation of hsa\_circ\_0005752 (Fig. 1B). After osteogenic differentiation for 7 days, we observed the increased ALP activity in hsa\_circ\_0005752 overexpressing group and markedly decreased in the hsa\_circ\_0005752 knockdown group, relative to the corresponding control group (Fig. 1C). The ARS staining indicated that mineralization was also significantly enhanced when hsa\_circ\_0005752 was overexpressed.

In contrast, hsa\_circ\_0005752 knockdown led to weaker mineralization (Fig. 1D). We also found osteogenic differentiation induced by OM for 7 days remarkably upregulated Runx2, ALP, Osx, and OCN, but downregulated p53. Additionally, hsa\_circ\_0005752 overexpression significantly increased the expressions of Runx2, ALP, Osx, OCN but remarkably decreased the expressions of p53 at mRNA and protein level (Fig. 1E-F). In contrast to hsa\_circ\_0005752 overexpressing, hsa\_circ\_0005752 knockdown exhibited the decreased levels of Runx2, ALP, Osx, and OCN as well as the increased p53 (Fig. 1E-F). Hsa\_circ\_0005752 overexpression promoted osteogenic differentiation of ADSCs, while hsa\_circ\_0005752 knockdown led to the inhibition of osteogenesis in ADSCs.

### 3.2. Hsa\_circ\_0005752 acted as a ceRNA of miR-496

To further characterize the underlying mechanisms by which hsa\_circ\_0005752 modulate the osteogenic differentiation of ADSCs, we first confirmed whether miR-496 participated in ADSC osteogenic differentiation [25]. Our data showed that miR-496 was dramatically downregulated, especially after OM inducing for 7 and

14 days (Fig. 2A). After transfecting pcDNA3.1-hsa\_circ\_0005752 or sh-hsa\_circ\_0005752 vector into ADSCs, miR-496 was significantly decreased when hsa\_circ\_0005752 was overexpressed but increased when hsa\_circ\_0005752 was silenced (Fig. 2B). The RNA pull-down assay found hsa\_circ\_0005752 was enriched by the Bio-WT-miR-496 rather than the Bio-MUT-miR-496 (Fig. 2C). To clarify their interaction between miR-496 and hsa\_circ\_0005752, we performed RIP assays in ADSCs transfected with miR-496 mimic and mimic-NC. Our data showed that anti-AGO2 enriched the hsa\_circ\_0005752 in the miR-496 overexpression group rather than in the control group (Fig. 2D). The bioinformatics analysis observed that miR-496 contained a binding sequence for hsa\_circ\_0005752 (Fig. 2E). The luciferase reporter assay further pointed out that miR-496 mimics significantly suppressed luciferase activity in the luciferase vector containing the WT-hsa\_circ\_0005752 sequence rather than the MUT-hsa\_circ\_0005752 sequence (Fig. 2E). All these data demonstrated that hsa\_circ\_0005752 directly targets miR-496.

### 3.3. miR-496 inhibited ADSCs osteogenic differentiation

To explore whether miR-496 is involved in ADSC's osteogenic differentiation, we transfected miR-496 mimics or inhibitors into ADSCs. Our results showed that relative to the corresponding control, miR-496 mimics enhanced miR-496 expression. In contrast, the miR-496 inhibitor diminished the miR-496 level (Fig. 3A). Further experiments pointed out that miR-496 overexpression suppressed OM-induced high ALP activity and the extracellular mineralization intensity, whereas miR-496 inhibitor enhanced the ALP activity and mineralization induced by OM (Fig. 3B-C). Finally, we found that miR-496 overexpression significantly attenuated OM-induced high levels of Runx2, ALP, Osx, and OCN and enhanced p53 expression (Fig. 3D-E). In contrast, miR-496 inhibition exhibited the opposite effects of miR-496 overexpression during osteogenic differentiation of ADSCs (Fig. 3D-E).

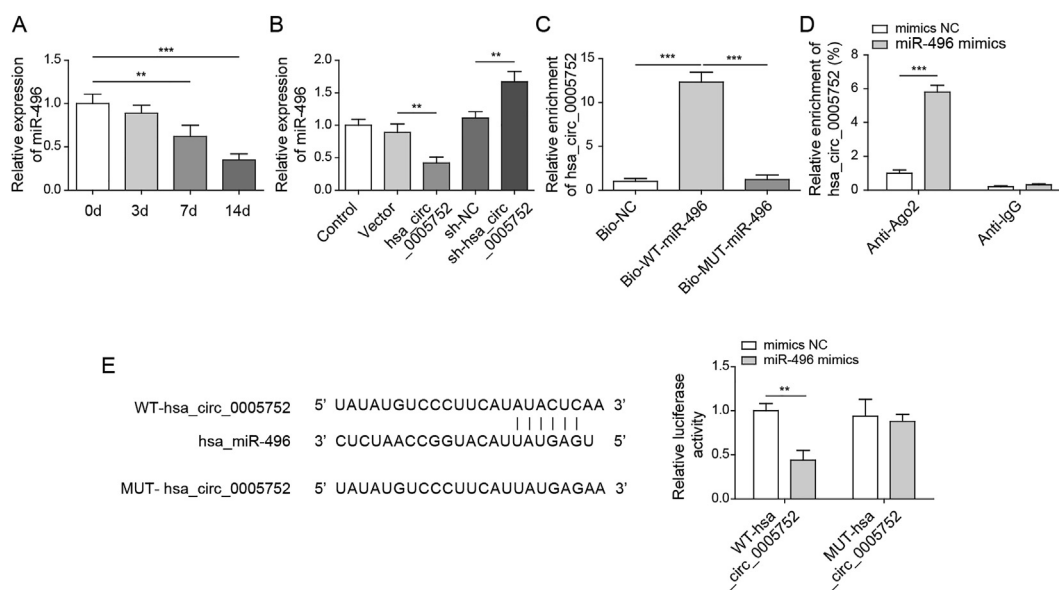


**Fig. 2. Hsa\_circ\_0005752 acted as a ceRNA of miR-496.** A: The miR-496 expression was measured by qRT-PCR during ADSCs osteogenic differentiation. B: The miR-496 expression was measured by qRT-PCR after transfections of hsa\_circ\_0005752, sh-hsa\_circ\_0005752, or their corresponding control. C: The enrichment of hsa\_circ\_0005752 was pull-downed by Biotin-WT-miR-496, rather than Biotin-MUT-miR-496 or Biotin- NC. D: The enrichment of hsa\_circ\_0005752 was analyzed by the RIP assays with anti-Ago2 or anti-IgG antibodies in ADSCs after transfected with miR-496 mimic or mimic-NC. E: The potential binding site between hsa\_circ\_0005752 and miR-496 was analyzed after co-transfection with WT-hsa\_circ\_0005752 or MUT-hsa\_circ\_0005752 luciferase reporter vectors with miR-496 mimic or mimic NC. Data indicated the mean ± SD, n = 3. \*\*P < 0.01, \*\*\*P < 0.01.

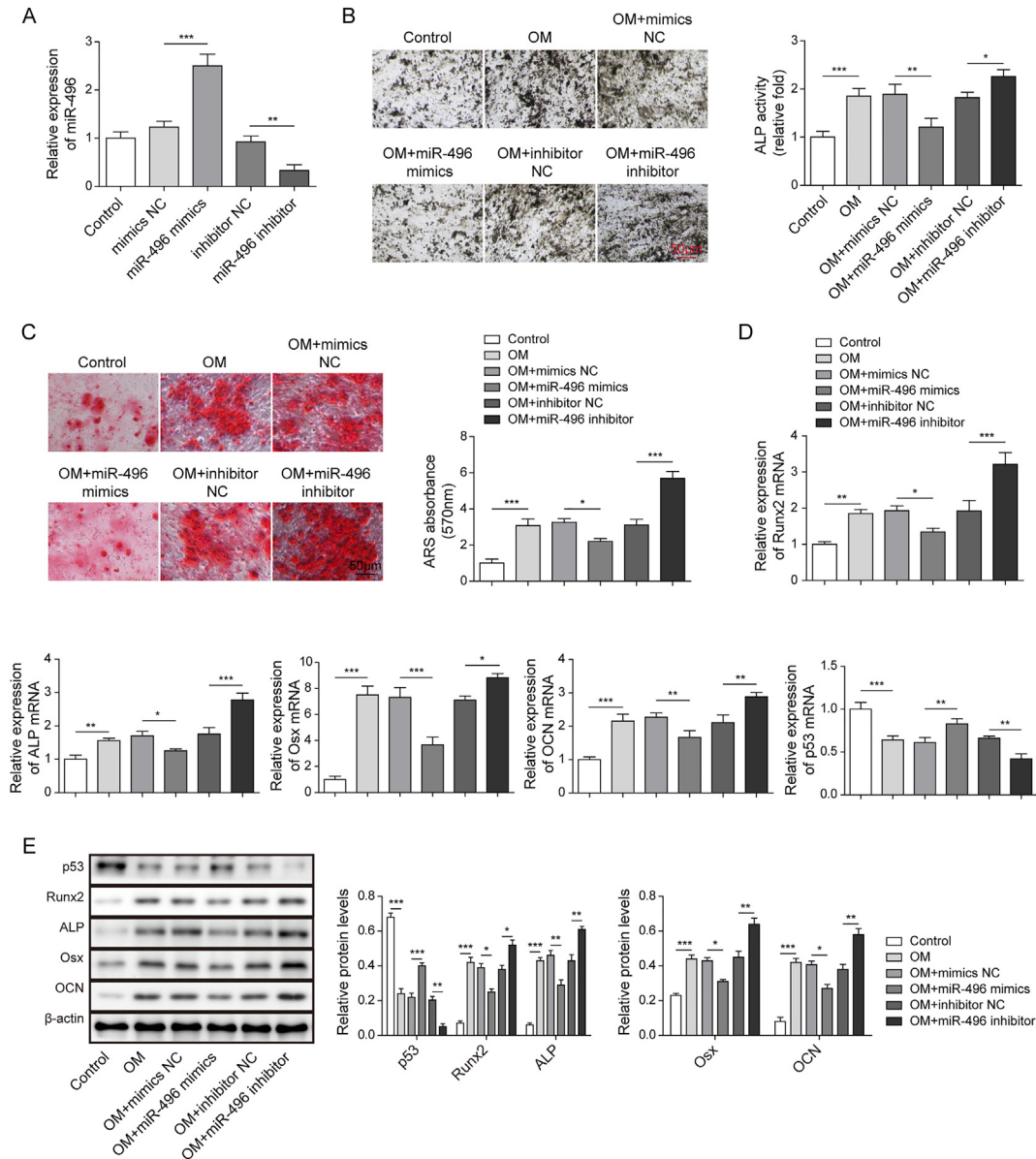


**Fig. 3. miR-496 inhibited ADSCs osteogenic differentiation.** A: The miR-496 expressions were detected by qRT-PCR after transfection of miR-496 mimics/inhibitors or individual control. B-C: Alkaline phosphatase (ALP) and the mineralization were determined by the ALP staining (B) or ARS staining (C). Scale bar = 50 μm. D-E: Runx2, ALP, Osx, OCN, and p53 mRNA levels were determined by qRT-PCR (D) or Western blot (E) in OM-treated ADSCs after miR-496 overexpression or knockdown. Data indicated the mean ± SD, n = 3. \*P < 0.05, \*\*P < 0.01, \*\*\*P < 0.01.

### 3.4. miR-496 directly targeted MDM2

From the above data, we confirmed that miR-496 was involved in OM-induced osteogenic differentiation of ADSCs. Further bioinformatics analysis predicted that there was a potential binding site in MDM2 for miR-496. Further studies showed that miR-496 mimics remarkably decreased the MDM2 at both mRNA and protein levels, but miR-496 inhibitors showed distinctly high levels of MDM2 (Fig. 4A-B). By the anti-Ago2 and anti-IgG RIP assay, we found that miRNA-496 overexpression could increase the adsorption of MDM2 mRNA on anti-Ago2 anti-Ago2 rather than by anti-IgG pull-down (Fig. 4C). By co-transfection of miRNAs and luciferase reporters, we found miR-496 exhibited a specific inhibition of

luciferase activity in the WT-MDM2 group, but no change of luciferase activity was found in the MUT-MDM2 group (Fig. 4D). All these data indicated that miR-496 could directly regulate MDM2 expression.

### 3.5. Hsa\_circ\_0005752 promoted ADSCs osteogenic differentiation through modulating MDM2 by miR-496

Accumulated evidence has shown that circRNAs functioned as miRNA sponges to influence the downstream target gene expression [14]. To explore the underlying mechanism of hsa\_circ\_0005752 during osteogenic differentiation, we co-transfected hsa\_circ\_0005752 overexpressing vector and miR-496 mimics or

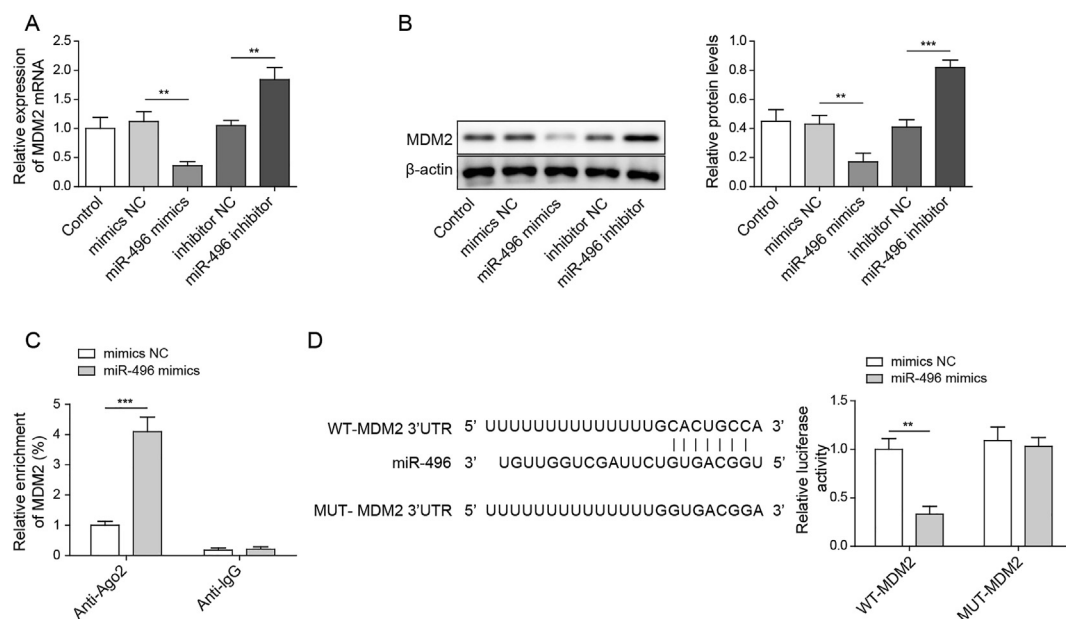


**Fig. 4. miR-496 directly targeted MDM2.** A and B: MDM2 expressions were detected by qRT-PCR (A) and Western blot (B) after miR-496 overexpression or knockdown. C: The enrichment of MDM2 to miR-496 was analyzed by the RIP assays with anti-Ago2 or anti-IgG antibodies in ADSCs after miR-496 overexpression or knockdown. D: A schematic diagram showed the alignment between miR-496 and WT- or MUT-MDM2. The relative luciferase activity was determined in ADSCs after miR-496 overexpression or knockdown. Data indicated the mean ± SD, n = 3. \*\*P < 0.01, \*\*\*P < 0.01.

sh-MDM2 into ADSCs after osteogenic medium (OM) induction. By qRT-PCR assay, we found that OM induction significantly inhibited miR-496 but upregulated MDM2 (Fig. 5A). Overexpressing hsa\_circ\_0005752 remarkably inhibited miR-496 and enhanced MDM2 under OM conditions. However, miR-496 mimics could rescue the effect of hsa\_circ\_0005752 overexpression on miR-496 and MDM2 expressions. When hsa\_circ\_0005752 overexpression vector was co-transfected with sh-MDM2, the high level of MDM2 induced by hsa\_circ\_0005752 overexpression was partially compromised (Fig. 5A). In the following experiments, we explored the role of the miR-496/MDM2 signaling pathway in osteogenic differentiation of hsa\_circ\_0005752 overexpressed ADSCs. Further experiments indicated that hsa\_circ\_0005752 overexpression markedly enhanced ADSC osteogenic differentiation by the increased ALP and mineralization. However, miR-496 overexpression or MDM2 knockdown could diminish the promoting effects of hsa\_circ\_0005752 overexpression (Fig. 5B-C). When hsa\_circ\_0005752 was overexpressed, osteogenic markers Runx2, ALP, Osx, OCN were remarkably enhanced, but p53 was significantly inhibited (Fig. 5D). However, miR-496 overexpression or MDM2 knockdown partially attenuated hsa\_circ\_0005752 on the expression of Runx2, ALP, Osx, OCN, and p53 (Fig. 5D). All those data indicated that miR-496 overexpression or MDM2 knockdown could attenuate the promoting effects of hsa\_circ\_0005752 on osteogenic differentiation.

### 3.6. RUNX3 regulated hsa\_circ\_0005752 expression during ADSCs osteogenic differentiation

To investigate whether RUNX3 could regulate osteogenic differentiation, we firstly detected the expression of RUNX3 during osteogenic differentiation of ADSCs. Our results revealed that RUNX3 was significantly upregulated during osteogenic

differentiation of ADSCs (Fig. 6A-B). CircBase (<http://circrna.org/>) dataset showed that hsa\_circ\_0005752 was generated from LPAR1. Interestingly, hTFtarget (<http://bioinfo.life.hust.edu.cn/hTFtarget>) found RUNX3 was a potential upper transcription factor for LPAR1. Then, we wonder whether RUNX3 could regulate hsa\_circ\_0005752 during osteogenic differentiation of ADSCs. To validate the potential binding ability of RUNX3 to LPAR1 promoter, we performed the ChIP-PCR assay and found the hsa\_circ\_0005752 coding gene LPAR1 was enriched abundantly in the DNA-protein complex by the RUNX3 antibody rather than IgG antibody (Fig. 6C), indicating RUNX3 bound to the LPAR1 promoter. Subsequently, we transfected the RUNX3 overexpressing vector, sh-RUNX3, or the corresponding empty vector with luciferase reporter vector pGL4.32-LPAR1 and measured the luciferase reporter activities. Our results revealed that RUNX3 overexpression enhanced the luciferase activity, but RUNX3 knockdown decreased the luciferase activity (Fig. 6D). Additional experiments pointed out that overexpression or knockdown of RUNX3 had no apparent effects on the protein level of LPAR1 (Fig. 6E). Besides, the level of hsa\_circ\_0005752 was positively correlated with RUNX3. Overexpression of RUNX3 significantly increased the hsa\_circ\_0005752 level, and the knockdown of RUNX3 decreased the hsa\_circ\_0005752 level (Fig. 6F). Taken together, we confirmed that RUNX3 mediated the level of hsa\_circ\_0005752.

### 3.7. RUNX3 promoted osteogenic differentiation of ADSCs via upregulating hsa\_circ\_0005752

Finally, we hope to clarify the effects of the RUNX3-hsa\_circ\_0005752 axis during the osteogenic differentiation of ADSCs. We performed the rescue experiments by overexpressing RUNX3 together with the hsa\_circ\_0005752 knockdown. As shown

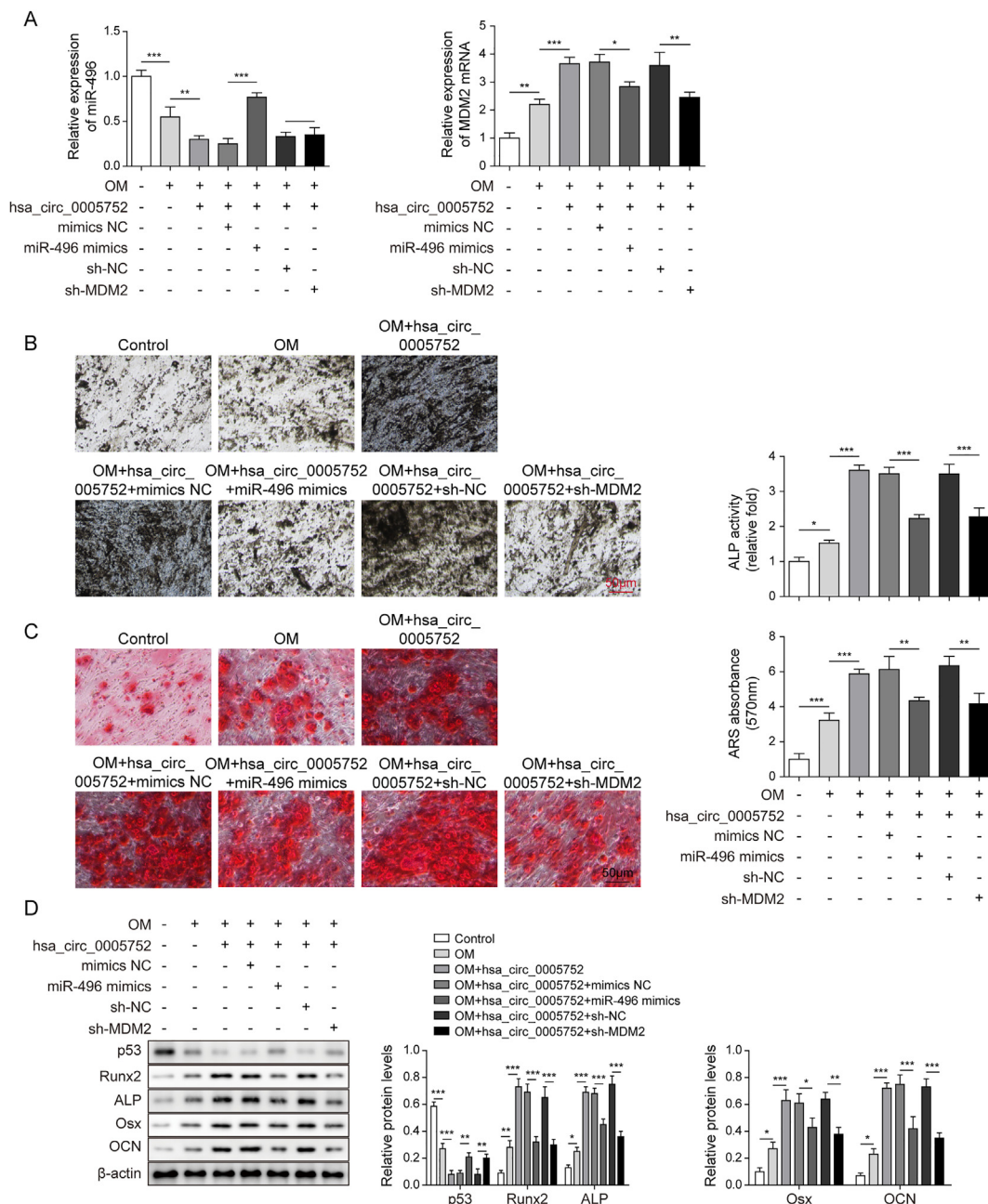


**Fig. 5. Hsa\_circ\_0005752 promoted ADSCs osteogenic differentiation through modulating MDM2 by miR-496.** A: miR-496 and MDM2 levels were detected by qRT-PCR in OM-induced ADSCs. B-C: The ALP staining (B) or ARS staining (C) determined ALP activity or mineralization. Scale bar = 50 μm. D: The p53, Runx2, ALP, Osx, OCN expression levels were measured by western blot. β-actin was used as an internal control. Data indicated the mean ± SD, n = 3. \*P < 0.05, \*\*P < 0.01, \*\*\*P < 0.001.

in Fig. 7A, we found OM treatment could upregulate both RUNX3 and hsa\_circ\_0005752. Meanwhile, overexpression of RUNX3 further enhanced the expression of RUNX3 and hsa\_circ\_0005752 in ADSCs. Knockdown of hsa\_circ\_0005752 did not influence the expression of RUNX3 but remarkably decreased the mRNA level of hsa\_circ\_0005752, indicating RUNX3 was an upper regulator. After OM-induced osteogenic differentiation, we found OM treatment increased both the ALP activity (Fig. 7B) and ARS staining intensity (Fig. 7C). Compared with OM treatment alone, RUNX3 overexpression induced significant enhancement of ALP and ARS staining intensity. However, knockdown of hsa\_circ\_0005752 could partially attenuate the distinct promoting effect of RUNX3 overexpression on osteogenic differentiation of ADSC.

Furthermore, western blot results showed OM treatment remarkably increased the levels of osteogenesis-related proteins MDM2, Runx2, ALP, Osx, OCN, and decreased p53 expression. Overexpressed RUNX3 effectively enhanced the osteogenic differentiation of ADSC by upregulating osteogenic marker proteins MDM2, Runx2, ALP, Osx, OCN, and decreasing p53. To investigate whether hsa\_circ\_0005752 knockdown could reverse the promoting osteogenic effects of RUNX3, we co-transfected ADSCs with RUNX3 overexpressing vector and hsa\_circ\_0005752 knockdown vector. As expected, the levels of osteogenesis-related proteins MDM2, Runx2, ALP, Osx, OCN significantly decreased, and p53 levels increased in RUNX3 overexpressing and sh-hsa\_circ\_0005752 group compared with RUNX3 overexpressing

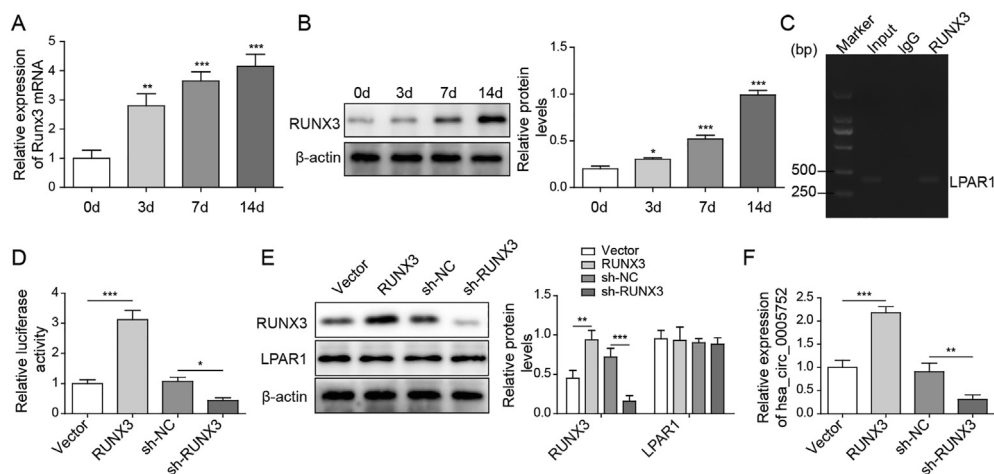


**Fig. 6.** RUNX3 regulated *hsa\_circ\_0005752* expression during ADSCs osteogenic differentiation. A–B. The RUNX3 mRNA or protein levels was detected in ADSCs after osteogenic differentiation for 0, 3, 7, and 14 days by qRT-PCR (A) or western blot (B). C. The binding capacity of RUNX3 to LAPR1 promoter was validated by the CHIP-qPCR experiment in ADSCs. D. The effects of RUNX3 on LAPR1 transcription were detected by luciferase reporter assay. E. The LPAR1 protein levels were detected in ADSCs after overexpressing or knockdown RUNX3 by western blot. F. The *hsa\_circ\_0005752* levels were detected in ADSCs after overexpressing or knockdown RUNX3 by qRT-PCR. Data indicated the mean  $\pm$  SD,  $n = 3$ . \* $P < 0.05$ , \*\* $P < 0.01$ , \*\*\* $P < 0.01$ .

and control vector group, suggesting that *hsa\_circ\_0005752* knockdown partially abolished the promoting effect of RUNX3 overexpression (Fig. 7D). These data suggested that RUNX3 mediated ADSCs osteogenic differentiation via upregulating *hsa\_circ\_0005752*.

#### 4. Discussions

Osteoporosis is featured by the decreased bone mass and increased skeletal fragility [26]. The etiologies for osteoporosis are multifactorial but closely related to smoking, family history of fracture, age (>65), and chronic diseases such as glucocorticoids, diabetes, rheumatoid arthritis [27]. Although the etiology is multifactorial, the imbalance between bone formation and bone resorption is one of the significant risk factors. The balance between bone regeneration and bone absorption is monitored in bone by stem/progenitor cells such as osteoblasts, osteocytes, and osteoclasts [28]. Therefore, the regulation of stem cells is significant revenue for managing the pathophysiological progress of osteoporosis. Previous studies showed that stem cell potential transplantation using the bioengineering scaffold method is an optimal stem-cell-based method to regulate *in vivo* osteogenesis effectively [29,30]. Osteoporosis is also a hereditary disease, so genetically modified stem cell delivery has provided an opportunity to prevent osteoporosis development [29]. Recently, circRNAs have been among the most promising molecules to regulate osteogenesis. This study focused on the expression and potential mechanisms of circRNA *hsa\_circ\_0005752* in ADSCs osteogenic differentiation during the progress of osteoporosis. We found that *hsa\_circ\_0005752* promoted *in vitro* osteogenic differentiation of ADSCs. Mechanically, *hsa\_circ\_0005752* could directly target miR-496 to regulate MDM2 expression. Also, miR-496 overexpression and MDM2 knockdown partially alleviated the effects of *hsa\_circ\_0005752* on osteogenic differentiation of ADSCs.

Previous studies confirmed that circRNAs were involved in many biological processes, including cell cycle, cellular signaling and stress, metabolism, normal embryonic development, and disease pathogenesis, including osteoarthritis [12,13]. It had been confirmed that the gene regulations by circRNAs were through several mechanisms, including acting as miRNA sponges and transcriptional or translational modifiers [12]. For example,

*hsa\_circRNA\_33287* promoted the osteogenic differentiation of maxillary sinus membrane stem cells by regulating the miR-124-3p/Runx3 pathway [17]. Circular RNA YAP1 suppressed the osteoporosis via sponging miR-376-3p to upregulate YAP1 and activate Wnt/ $\beta$ -catenin signaling to promote osteogenic differentiation [30]. A recent study using circRNA microarray analysis found that 290 circRNAs were differentially expressed after osteogenic differentiation [18]. Further experiment validated that *hsa\_circ\_0005752* was highly regulated, indicating that *hsa\_circ\_0005752* might play an essential role in osteogenic differentiation ADSCs. However, the definite mechanism of *hsa\_circ\_0005752* in osteogenic differentiation remains unclear. Here, we firstly confirmed that *hsa\_circ\_0005752* overexpression could promote osteogenic differentiation of ADSCs. Further experiments pointed out that *hsa\_circ\_0005752* could directly bind to and inhibit miR-496. These findings suggested that *hsa\_circ\_0005752* promotes osteogenic differentiation, possibly via regulating miR-496.

A previous study exhibited that the pro-inflammatory cytokine IL-1 $\beta$  could activate miR-496 and subsequently inhibit bone mineralization and osteogenic marker genes (Runx2 and Osx) [31]. Furthermore, a recent experiment showed that miR-496 inhibition significantly increased RUNX2 and OCN during osteogenic differentiation of human dental pulp stem cells (hDPSCs) [25]. All these studies hinted that miR-496 was an active regulator for osteogenic differentiation. Our study found that miR-496 overexpression inhibited osteogenic differentiation and decreased osteogenic differentiation markers Runx2, ALP, Osx, and OCN. Using the bioinformatics method, we found that MDM2 3' UTR contained a complementary binding sequence of miR-496. Next, our RIP and Luciferase reporter assay data showed that miR-496 directly targeted MDM2 and inhibited its expression, while the MDM2-p53 pathway could regulate the osteogenic differentiation [21]. Our study first found that *hsa\_circ\_0005752* mediated ADSCs osteogenic differentiation through regulating MDM2/p53 pathway by miR-496.

Previous reports confirmed that RUNX3 played a pivotal role in osteogenic differentiation [17,32,33]. RUNX3 could act as a transcription factor to regulate gene transcription. Klunker et al. shown that RUNX3 could bind to the promoter of Foxp3 and regulate Foxp3 expression [34]. Our study performed bioinformatics analysis using hTFtarget (<http://bioinfo.life.hust.edu.cn/>)

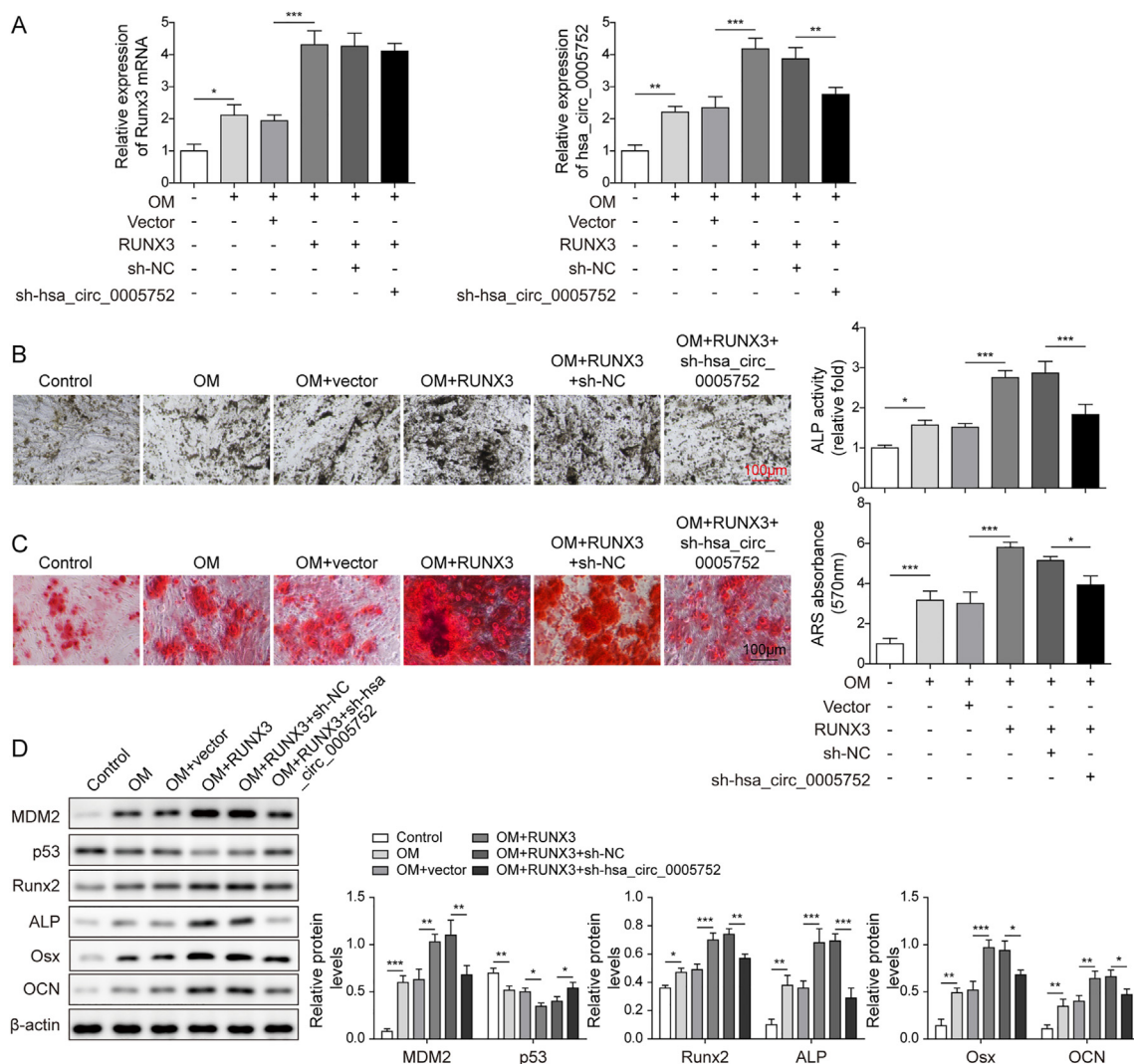


**Fig. 7. RUNX3 promoted osteogenic differentiation of ADSCs via upregulating hsa\_circ\_0005752.** A. The mRNA levels of RUNX3 and hsa\_circ\_0005752 were determined by qRT-PCR in OM-induced ADSCs after transfection with pcDNA3.1 empty vector, pcDNA3.1-RUNX3 single or together with sh-NC or sh- hsa\_circ\_0005752. B-C. The osteogenic differentiation was assessed by the ALP staining (B), and ARS staining (C) in OM-induced ADSCs after transfection with pcDNA3.1 empty vector or pcDNA3.1-RUNX3 single or together with sh-NC or sh- hsa\_circ\_0005752. D. The protein levels (MDM2, p53, Runx2, ALP, Osx, and OCN) were measured by western blot in OM-induced ADSCs after transfection with pcDNA3.1 empty vector, pcDNA3.1-RUNX3 single or together with sh-NC or sh- hsa\_circ\_0005752. Data indicated the mean  $\pm$  SD, n = 3. \*P < 0.05, \*\*P < 0.01, \*\*\*P < 0.01.

hTFtarget) and found RUNX3 is potentially bound to the LPAR1 promoter. Further, the ChIP-PCR and luciferase reporter assays identified that RUNX3 directly bound to the promoter of LPAR1 and enhanced the expression of LPAR1 at mRNA level rather than at protein level. Meanwhile, overexpression of RUNX3 upregulated the expression of hsa\_circ\_0005752. On the contrary, the knockdown of RUNX3 decreased the level of hsa\_circ\_0005752. Furthermore, RUNX3 promoted osteogenic differentiation, which was attenuated by hsa\_circ\_0005752 knockdown. All those experiments elucidated that RUNX3 enhanced osteogenic differentiation of ADSCs via modulating hsa\_circ\_0005752/miR-496/MDM2-p53 pathway.

In conclusion, we confirmed that hsa\_circ\_0005752/miR-496/MDM2 acted as a ceRNA loop to facilitate the osteogenic differentiation, indicating hsa\_circ\_0005752 might be a novel therapeutic avenue for the therapeutics of osteoporosis. Importantly, RUNX3 as a transcriptional factor could directly regulate the transcriptional progress of LPAR1, thus upregulated hsa\_circ\_0005752 and contributed to ADSCs' osteogenic differentiation. However, a circRNA can act as a transcriptional or translational regulator to regulate multiple miRNA expression, so

the definite function of hsa\_circ\_0005752 should be further investigated in the future.

**Funding**

This work was supported by Hunan Provincial Health Commission (No. C2019108).

**Availability of data and materials**

All data collected and analyzed during the current study are available from the corresponding author on reasonable request.

**Ethics approval and consent to participate**

Not applicable.

**Consent for publication**

All the authors approved the publication.

## Declaration of competing interest

The authors declare that they have no competing interests to disclose.

## Acknowledgments

Not applicable.

## References

- [1] Compston JE, McClung MR, Leslie WD. Osteoporosis. *Lancet* 2019;393(10169):364–76.
- [2] Wu QY, Li X, Miao ZN, Ye JX, Wang B, Zhang F, et al. Long non-coding RNAs: a new regulatory code for osteoporosis. *Front Endocrinol (Lausanne)* 2018;9:587.
- [3] Mazini L, Rochette L, Amine M, Malka G. Regenerative capacity of adipose derived stem cells (ADSCs), comparison with mesenchymal stem cells (MSCs). *Int J Mol Sci* 2019;20(10).
- [4] Paspaliaris V, Kolios G. Stem cells in osteoporosis: from biology to new therapeutic approaches. *Stem Cell Int* 2019;2019:1730978.
- [5] Barba M, Di Taranto G, Lattanzi W. Adipose-derived stem cell therapies for bone regeneration. *Expert Opin Biol Ther* 2017;17(6):677–89.
- [6] Lee SH, Hyeon DY, Yoon SH, Jeong JH, Han SM, Jang JW, et al. RUNX3 methylation drives hypoxia-induced cell proliferation and antiapoptosis in early tumorigenesis. *Cell Death Differ* 2021;28(4):1251–69.
- [7] Hantisteanu S, Dicken Y, Negreanu V, Goldenberg D, Brenner O, Leshkowitz D, et al. Runx3 prevents spontaneous colitis by directing the differentiation of anti-inflammatory mononuclear phagocytes. *PLoS One* 2020;15(5):e0233044.
- [8] Li Y, Li H, Han J. Sphingosine-1-phosphate receptor 2 modulates pain sensitivity by suppressing the ROS-RUNX3 pathway in a rat model of neuropathy. *J Cell Physiol* 2020;235(4):3864–73.
- [9] Mevel R, Draper JE, Lie-A-Ling M, Kouskoff V, Lacaud G. RUNX transcription factors: orchestrators of development. *Development* 2019;146(17).
- [10] Soung do Y, Dong YF, Wang YJ, Zuscik MJ, Schwarz EM, O'Keefe RJ, et al. Runx3/AML2/Cbfa3 regulates early and late chondrocyte differentiation. *J Bone Miner Res* 2007;22(8):1260–70.
- [11] Choo SY, Yoon SH, Lee DJ, Lee SH, Li K, Koo IH, et al. Runx3 inhibits endothelial progenitor cell differentiation and function via suppression of HIF-1 $\alpha$  activity. *Int J Oncol* 2019;54(4):1327–36.
- [12] Haque S, Harries LW. Circular RNAs (circRNAs) in Health and disease. *Genes (Basel)* 2017;8(12).
- [13] Shang Q, Yang Z, Jia RB, Ge SF. The novel roles of circRNAs in human cancer. *Mol Canc* 2019;18(1):6.
- [14] Hansen TB, Jensen TI, Clausen BH, Bramsen JB, Finsen B, Damgaard CK, et al. Natural RNA circles function as efficient microRNA sponges. *Nature* 2013;495(7441):384–8.
- [15] Salzman J. Circular RNA expression: its potential regulation and function. *Trends Genet* 2016;32(5):309–16.
- [16] Yu L, Liu Y. circRNA\_0016624 could sponge miR-98 to regulate BMP2 expression in postmenopausal osteoporosis. *Biochem Biophys Res Commun* 2019;516(2):546–50.
- [17] Peng W, Zhu SX, Chen JL, Wang J, Rong Q, Chen SL. Hsa\_circRNA\_33287 promotes the osteogenic differentiation of maxillary sinus membrane stem cells via miR-214-3p/Runx3. *Biomed Pharmacother* 2019;109:1709–17.
- [18] Kang Y, Guo S, Sun Q, Zhang T, Liu J, He D. Differential circular RNA expression profiling during osteogenic differentiation in human adipose-derived stem cells. *Epigenomics* 2020;12(4):289–302.
- [19] Moll UM, Petrenko O. The MDM2-p53 interaction. *Mol Canc Res* 2003;1(14):1001–8.
- [20] Zheng H, Yang G, Fu J, Chen Z, Yuan G. Mdm2 promotes odontoblast-like differentiation by ubiquitinating Dlx3 and p53. *J Dent Res* 2020;99(3):320–8.
- [21] Lengner CJ, Steinman HA, Gagnon J, Smith TW, Henderson JE, Kream BE, et al. Osteoblast differentiation and skeletal development are regulated by Mdm2-p53 signaling. *J Cell Biol* 2006;172(6):909–21.
- [22] Daniele S, Giacomelli C, Pietrobono D, Barresi E, Piccarducci R, Pietra VL, et al. Long lasting inhibition of Mdm2-p53 interaction potentiates mesenchymal stem cell differentiation into osteoblasts. *Biochim Biophys Acta Mol Cell Res* 2019;1866(5):737–49.
- [23] Fu D, Lala-Tabbert N, Lee H, Wiper-Bergeron N. Mdm2 promotes myogenesis through the ubiquitination and degradation of CCAAT/enhancer-binding protein beta. *J Biol Chem* 2015;290(16):10200–7.
- [24] Hallenborg P, Feddersen S, Francoz S, Murano I, Sundekilde U, Petersen RK, et al. Mdm2 controls CREB-dependent transactivation and initiation of adipocyte differentiation. *Cell Death Differ* 2012;19(8):1381–9.
- [25] Ji F, Pan J, Shen ZC, Yang Z, Wang J, Bai XB, et al. The circular RNA circRNA124534 promotes osteogenic differentiation of human dental pulp stem cells through modulation of the miR-496/beta-Catenin pathway. *Front Cell Dev Biol* 2020;8:230.
- [26] Ensrud KE, Crandall CJ. Osteoporosis. *Ann Intern Med* 2017;167(3):ITC17–32.
- [27] Rosen CJ. In: Endotext KR Feingold, et al., editors. The epidemiology and pathogenesis of osteoporosis; 2000. South Dartmouth (MA).
- [28] Yang TL, Shen H, Liu A, Dong SS, Zhang L, Deng FY, et al. A road map for understanding molecular and genetic determinants of osteoporosis. *Nat Rev Endocrinol* 2020;16(2):91–103.
- [29] Ralston SH. Genetic control of susceptibility to osteoporosis. *J Clin Endocrinol Metab* 2002;87(6):2460–6.
- [30] Huang Y, Xiao D, Huang SH, Zhuang JX, Zheng XQ, Chang YB, et al. Circular RNA YAP1 attenuates osteoporosis through up-regulation of YAP1 and activation of Wnt/beta-catenin pathway. *Biomed Pharmacother* 2020;129:110365.
- [31] Huang J, Chen L. IL-1 $\beta$  inhibits osteogenesis of human bone marrow-derived mesenchymal stem cells by activating FoxD3/microRNA-496 to repress wnt signaling. *Genesis* 2017;55(7).
- [32] Wang Y, Feng QL, Ji CX, Liu XH, Li L, Luo JY. RUNX3 plays an important role in mediating the BMP9-induced osteogenic differentiation of mesenchymal stem cells. *Int J Mol Med* 2017;40(6):1991–9.
- [33] Saito T, Ohba S, Yano F, Seto I, Yonehara Y, Takato T, et al. Runx1 and Runx3 are downstream effectors of Nanog in promoting osteogenic differentiation of the mouse mesenchymal cell line C3H10T1/2. *Cell Reprogr* 2015;17(3):227–34.
- [34] Klunker S, Chong MMW, Mantel PY, Palomares O, Bassin C, Ziegler M, et al. Transcription factors RUNX1 and RUNX3 in the induction and suppressive function of Foxp3+ inducible regulatory T cells. *J Exp Med* 2009;206(12):2701–15.